

An investigation into the mechanics of fiber reinforced composite disk springs

Peng Yang, Stacy Van Dyke and Rani F. Elhajjar *¹

Department of Civil Engineering and Mechanics, College of Engineering and Applied Science, University of Wisconsin-Milwaukee, 3200 N Cramer Street, Milwaukee, Wisconsin, 53211 USA

(Received November 07, 2013, Revised September 12, 2014, Accepted September 26, 2014)

Abstract. An analytical and experimental investigation is performed into the mechanical behavior of carbon-fiber/epoxy woven coned annular disk springs. An analytical approach is presented for predicting the deformation behavior of disk springs of specially orthotropic laminates with arbitrary geometric parameters. In addition, an analytical methodology is proposed for obtaining the deformation behavior of a stack of disk springs. The methodology is capable of accounting for parallel and series arrangements for uniform and irregular stacks. Element and assembly experimental results are used to validate the proposed method showing how to achieve flexible spring rates at various deflections ranges. This manuscript also provides guidelines for design and validation of disk spring assemblies.

Keywords: nonlinear disk springs; mechanical behavior; manufacturing; specially orthotropic materials; structural behavior

1. Introduction

Since the introduction of fiber reinforced composites, researchers have been quick to investigate the various possibilities of incorporating them in mechanical springs. Fiber composites give the possibility to optimize the design of the structure by aligning the high strength fibers in the direction of highest stresses. For example, Cho *et al.* have shown in this journal how optimum design can be achieved in fiber-reinforced tire belt structure (Cho *et al.* 2013). This motivation was driven by the possibility of robust light-weight replacements of metallic components. Elliptical springs comprising layers of composite materials arranged in non-uniform longitudinal dimensions can be used to obtain spring behavior (Mallick 1985, Huchette and Hall Jr. 1976). Mahdi *et al.* (2006) investigated the use of the elliptical spring configurations using woven roving composites. They demonstrated the influence of the ellipticity ratio on the spring rate and the performance of the springs through the failure history. The use of nickel–titanium alloy wires in altering the spring rates at elevated temperatures in composite circular rings was also investigated (Wong *et al.* 2004). Tse *et al.* (1994) investigated the behavior of composite circular rings under uniaxial compression using the equivalent flexural rigidity approach. In another approach they investigated the stress and strain distributions of a mid-plane symmetric laminated circular ring under uniaxial loading

*Corresponding author, Professor, E-mail: elhajjar@uwm.edu

using a strain energy approach (So *et al.* 1991). Chiu *et al.* (2009) studied the fatigue behavior of hybrid helical composites springs. Composite materials have also been proposed to create high-energy, compact storage in composite sulcated springs (Scowen and Hughes 1985, Thompson *et al.* 1992). In a sulcated spring, an elongated strip of composite materials is arranged in a zig-zag fashion acting as a flexible spring element. Leaf springs have also been proposed using composites (Suprith *et al.* 2013, Subramanian and Senthilvelan 2011). Composite coil springs using carbon fiber have also been investigated for weight reduction purposes under static and dynamic conditions (Hendry and Probert 1986, Çalim 2009, Hwan *et al.* 2010). However, the challenge in these is in controlling the interlaminar stresses produced during compression of the springs. Additional challenges in helical springs also relate to the effects of warping on the natural frequencies (Yu and Hao 2013). Other researchers have also investigated the fiber paths in composite conical shells under compression (Naderi *et al.* 2014, Topal 2013). Their results showed that the tailoring of fibers in the composite can improve the composite buckling strength.

Stacks of composite disk springs have also been proposed to achieve spring behavior. In this implementation, composite disk springs are proposed taking advantage of the superior behavior of composites under flexural loading conditions. The springs are assembled in parallel or series combinations to achieve various spring rate and deflection characteristics. The development of disk springs can be traced to the early work by Almen and Laszlo (1936) who presented formulas for the load-deflection characteristics of cone shaped annular disk springs with particular application to metal disc springs with linear elastic material behavior. Curti and Montanini (1999) studied the effect of friction on the behavior of composite disk springs. The effect of material nonlinearity on the load-deflection curve and the stress field in disc springs was investigated to resolve some of the contradictions in the analytical presentations (Curti and Raffa 1992). Dharan and Bauman (2007) presented an experimental investigation of several prototype disk springs and compared the results to comparable steel springs. The design equations for steel disk springs were modified for a quasi-isotropic composite lay-up. Several prototype disc springs were manufactured and tested, and compared with the performance of equivalent steel springs. The flexibility of disk springs allows for customization of spring stiffnesses to suit different applications. The mechanical deformation in disk springs is primarily in flexure, contrast this with the large interlaminar stress conditions produced when spiral springs are used where multi-mode deformation modes such as torsion are seen to occur. Significant weight savings can be realized using disk springs by using materials with high specific stiffness and strength. The disk spring stacks also benefit from the inherent flexibility in fiber reinforced composite design.

In this study, an analytical and experimental investigation is performed into the mechanical behavior of initially coned annular fiber reinforced composite disk springs. A carbon-fiber/epoxy woven composite is used to validate an analytical approach for these springs incorporating the material properties of specially orthotropic laminates. We also present a method to determine the linear and nonlinear behavior of even and non-even spring stacks containing the series and parallel elements. The design of the spring stack is typically performed in two parts. The first is the design of a single disk and the second is the design and arrangement of the spring stack comprising various units.

2. Analytical model

The development of the analytical method for characterizing the spring deformation is divided into two sections. The first portion involves characterization of the individual disk springs

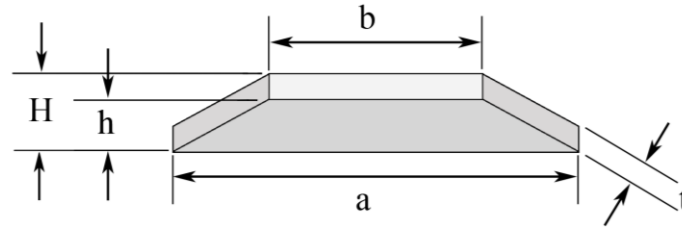


Fig. 1 Schematic of disk spring showing all the key dimensions

extending from the original equations derived by Almen and Laszlo (1936) for specially orthotropic cross-ply laminates. This is followed by an approach to couple the stiffness contributions of parallel and series arrangements of the individual disk elements to the entire stack assembly. The load versus deflection relationship in a single annular-disk spring loaded at the inner edge and supported by the outer edge, is governed by the following relation (Fig. 1) (Almen and Laszlo 1936)

$$P = \frac{E\delta}{(1-\nu^2)Ma^2} \left[(h-\delta) \left(h - \frac{\delta}{2} \right) t + t^3 \right] \quad (1)$$

where P is the axial load, E is the modulus of elasticity, δ is the axial deflection, ν is the Poisson's ratio, h is the free height of the disk, t is the thickness, a is the outer radius of the disk. In this equation, the constant M is a function of α , the ratio of the outer to inner radius, ($\alpha = a / b$)

$$M = \frac{6 \left[\frac{(\alpha-1)}{\alpha} \right]^2}{\pi \ln \alpha} \quad (2)$$

In the case of a specially orthotropic laminate, the laminate bending moduli and Poisson ratio are used and can be determined by

$$E_x^b = \frac{12(D_{11}D_{22} - D_{12}^2)}{t^3 D_{22}} \quad (3)$$

$$E_y^b = \frac{12(D_{11}D_{22} - D_{12}^2)}{t^3 D_{11}} \quad (4)$$

$$G_{xy}^b = \frac{12D_{66}}{t^3} \quad (5)$$

$$\nu_{xy}^b = \frac{D_{12}}{D_{22}} \quad (6)$$

where the D_{11} , D_{12} , D_{22} and D_{66} are coefficients from the bending stiffness matrix obtained from the classical lamination plate theory. The modulus in Eq. 1 is modified to account for the average modulus for the disk spring. In composite laminates and specifically orthotropic laminates, the

elastic modulus, E will vary depending on the angle, θ , away from the primary axis

$$E(\theta) = \left[\frac{m(\theta)^2}{E_x^b} (m(\theta)^2 - n(\theta)^2 \nu_{xy}^b) + \frac{n(\theta)^2}{E_y^b} (n(\theta)^2 - m(\theta)^2 \nu_{xy}^b) + \frac{m(\theta)^2 n(\theta)^2}{G_{xy}^b} \right]^{-1} \quad (7)$$

To account for the changing modulus, the modulus in Eq. (1) is modified to the average modulus for the disk spring, E_{ds} , which is found by integrating Eq. (7) around the spring boundary to obtain

$$E_{ds} = \frac{1}{2\pi} \int_0^{2\pi} E(\theta) d\theta \quad (8)$$

Substituting this into Eq. (1) yields a new equation for the load versus deflection of the composite disk spring of a specially orthotropic composite

$$P = \frac{E_{ds} \delta}{(1-\nu^2)Ma^2} \left[(h-\delta) \left(h - \frac{\delta}{2} \right) t + t^3 \right] \quad (9)$$

Similarly, the instantaneous spring rate, r , and strain energy, V can be expressed as

$$r(\delta) = \frac{E_{ds} t}{(1-\nu^2)Ma^2} \left[(h^2 - 3\delta h) + \frac{3\delta^2}{2} + t^2 \right] \quad (10)$$

$$V(\delta) = \frac{E_{ds} \delta^2}{2(1-\nu^2)Ma^2} \left[t \left(h - \frac{\delta}{2} \right)^2 + t^2 \right] \quad (11)$$

Individual disk springs, or elements, can be arranged and grouped as described in Fig. 2. A group of two or more elements in parallel is a unit. A group of two or more units in series is a stack. The orientation and number of units in a stack alter the stiffness and load bearing capacity as

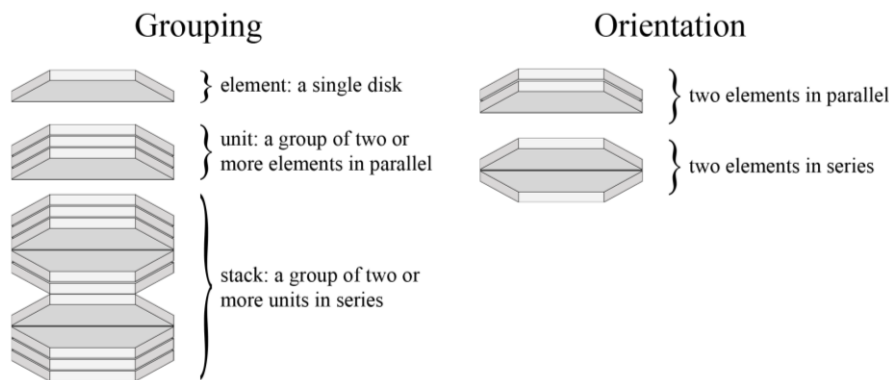


Fig. 2 Terminology in a disk spring assembly

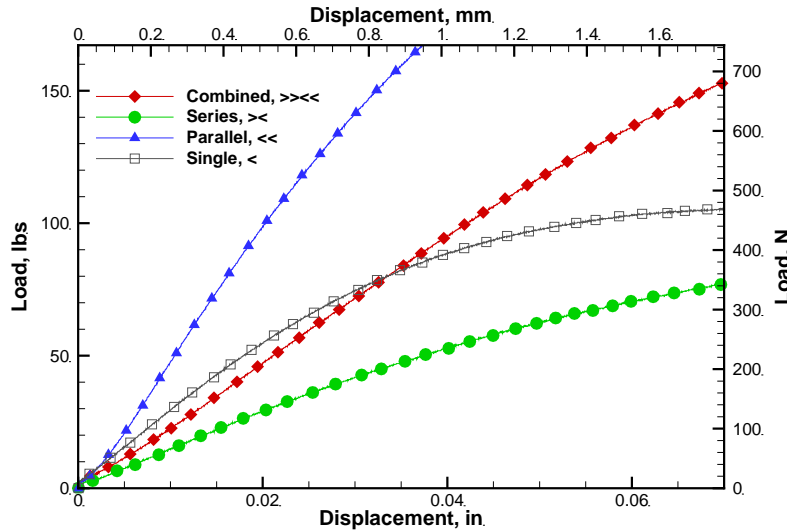


Fig. 3 Effect of series and parallel arrangements on spring deflection (experimental results)

shown in Fig. 3. When elements are stacked in parallel, the maximum loading capacity of the assembly is the addition of its individual elements but the deflection of the assembly is the same as that of a single element. For a series configuration, the maximum load is equal to a single elements but the maximum deflection of the assembly is equal to the maximum deflection of the elements combined. Since many practical applications require a large number of disks in each spring stack, a short hand notation was developed to designate how the stack is presented. Chevron brackets (“<” or “>”) maybe used to represent a limited number of springs, but it quickly gets difficult to account for a large number of disks using this notation. The alternative notation works as follows. Starting at the bottom of the stack, count the number of elements in each unit of adjacent parallel disk springs. Separate each unit by a dash symbol “-” to indicate that they are in a series combination. For example, the combination of disks represented with chevron brackets (<< > <<< >>) will have the notation “2-1-3-2”. Next, indicate the orientation of the starting spring using the chevron symbols “<” or “>”. For example, a group of two parallel springs in series with a group of three parallel springs can have the notation “< 2-3” << >>>” or “> 2-3” (>> <<<) depending on the orientation. If there is a reoccurring sequence in the stack, bracket the reoccurring sequence and indicate the number of them using a subscript. There are two type of sequences used: repeating and symmetrical. If the sequence is repeating, use an “r” in the subscript of the stack notation. For example, (<< >>> << >>>) has the notation of “(< 2-3)_{2r}”. If the sequence is symmetric about the center of the stack, indicate this using an “s” in the subscript notation. For example, (<< >>> <<< >>>) will be notated as “(< 2-3)_{2s}”.

The linear behavior of a spring stack is determined using an analogy to the analysis of electrical resistors. The equation to describe the spring constant of the entire stack, K_{total} and the height of the overall stack, L , are given by Schnorr (2003)

$$K_{total} = \left(\frac{N_s}{N_p K} \right)^{-1} \tag{12}$$

$$L = N_s[H + (N_p - 1)t] \quad (13)$$

where K is the spring constant of a single disk element, N_p is the number of elements in a unit, N_s is the number of units stacked in series. H is the total height of a single disk ($h + t$), and t is the thickness of a single disk. Substituting Eq. (12) into Eq. (13) in terms of either N_p or N_s will produce the number of disks and stacking direction needed to achieve the desired stiffness in the desired height of the overall stack, L . Eqs. (12) and (13) can be used to determine the stiffness when all the units in a stack contain the same number of elements. The equations above are limited in their assumption of linear load-displacement behaviors. There may be situations where a progressively higher stiffness is needed with increased deflection or where a bump-stop action is desired. This design requires a more precise approach to characterize the non-linear load-deflection behavior of a stack of disk springs.

Different flattening “stages” occur within a stack when its units do not all have the same number of elements. As a stack is loaded, each unit will carry the same load, but the deflection within each is dependent on that specific stiffness of each unit. Stage zero describes the compression of the stack while none of the disks have been fully compressed. Stage one begins when all of the units with a single disk are completely compressed. Stage two begins when the units with two disks are completely compressed and so on. A new stage begins at the maximum deflection of the previous stage. For example, a stacking sequence (< 1-1-2) will have 3 units (1, 1, and 2) and two stages of compression. During stage zero the stack will experience deflection, but none of the disks will be fully compressed. Because the (< 1-1) section of the stack has a higher compression rate and lower stiffness than the (< 2) section, it will fully compress first with a deflection of $2h$. The compression of the “1 element units” signifies the start of stage one. During stage one, the (< 2) section of the stack will continue to compress to a maximum deflection of h . When this is complete, the stack will be fully compressed. The equation to characterize the load-displacement curve of a stack of disk springs extends from Eq. (1). When Eq. (1) is plotted, it shows the load-displacement profile for a single disk *element*. The proposed approach will be similar, but instead of a single element being graphed, every *unit* will be graphed. Using Eqs. (1) and (12), each unit’s load-deflection profile is defined by

$$P\left(\delta, \frac{K_t}{K_i}, x_{st}, N_{pi}\right) = \frac{E\delta'}{(1-\nu^2)Ma^2} \left[(h - \delta') \left(h - \frac{\delta'}{2} \right) t + t^3 \right] N_{pi} \quad (14)$$

where δ' and x_{st} are determined by

$$\delta' = (\delta - x_{st}) \frac{K_t}{K_i} \quad (15)$$

$$x_{st} = Uh \quad (16)$$

where x_{st} is equal to the number of units with the same number of elements that are already flattened, U , multiplied by the free height of a single disk, h . The variable x_{st} is the compressible height of the previous stage used to offset the next stage. Therefore, x_{st} is zero during stage zero loading because no disk has completely flattened. N_{pi} is the number of elements in the i th unit, and K_t / K_i is a stiffness ratio which determines the compression rate of the i th unit compared to the overall stack.

The load-deformation curves for each unit are then used to construct a load-deflection profile for each stage. The load-deflection profile of each stage is determined by taking the average of the unit profiles still compressing during that stage

$$P_s = \sum_{i=1}^n \frac{\left(\delta, \frac{K_i}{K_i}, x_{st}, N_{pi}\right)}{n} \tag{17}$$

P_s is the load-deflection and the subscript “ s ” indicates the number of flattening stages, n is the number of units in the stack. The following example illustrates this process. In the stacking sequence of (< 1-1-2), assuming a free height of 2.4 mm (0.093 in), we can create its load-displacement graph using Eqs. (14) and (17). A load-displacement profile is generated for every stage a stack experiences. The number of stages is equal to the number of *types* of units. When the profiles for each stage are complete, they are combined to form the overall stack load-displacement profile. Since there are only two *types* of units in this example (i.e., 1 and 2 element units), there will be two stages. Fig. 4(a) shows the load-displacement profile for stage

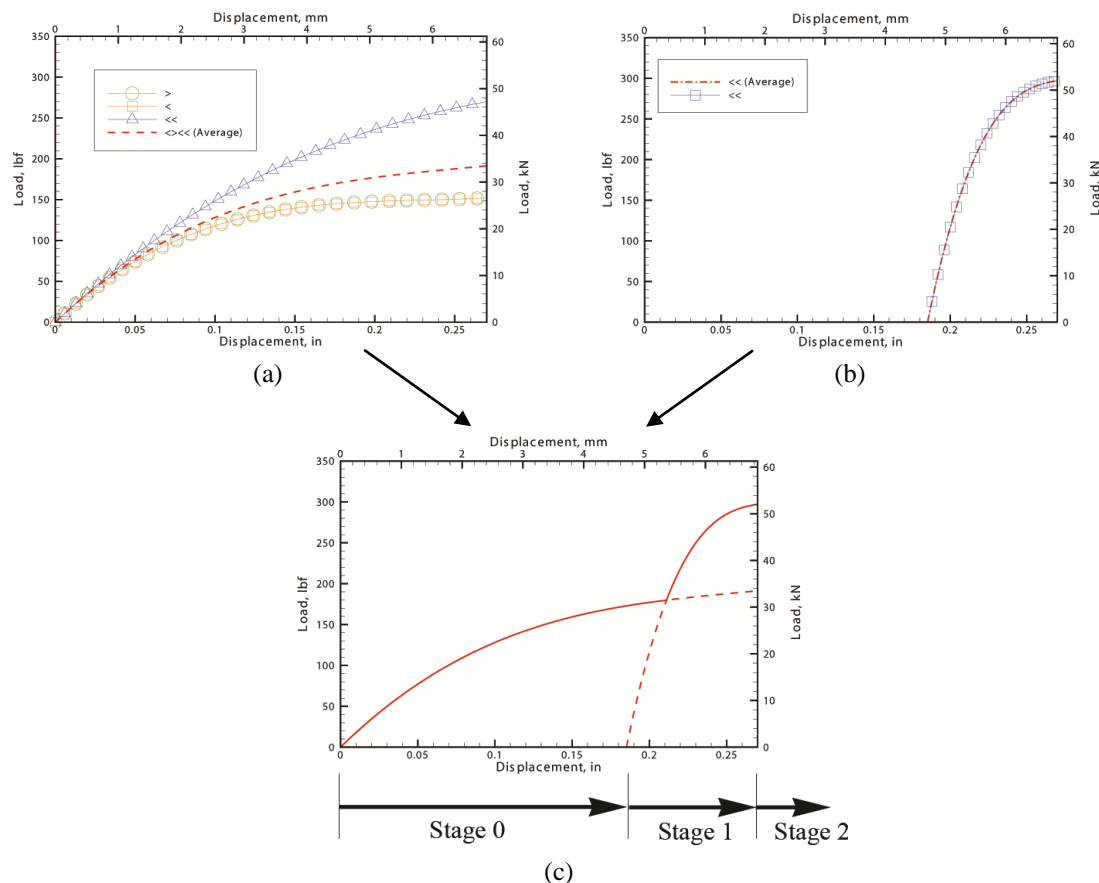


Fig. 4 (a) All the units in stage zero compression and their average; (b) the unit in stage one compression and its average; (c) combination of stage zero and stage one compression to form the load-displacement profile of the stack. The solid line is the effective curve.

zero, when none of the units have fully compressed. All three unit profiles are graphed using Eq. (14). The average of all three unit profiles (Eq. (17)) is the overall stack load-displacement profile in stage zero. Fig. 4(b) shows the stage one profiles. During stage one, the “1 element units” have fully compressed and only the “2 element unit” continues to deflect. Because this is the only unit still compressing, the overall stack profile is the same as the 2 element unit curve in stage one. Fig. 4(c) combines the stage zero and stage one average profiles together. The resulting graph shows two lines intersecting one another. The solid lines are the effective curve which is used to describe the characteristics of the stack. The intersection point is the transition from one stage to another. It should be noted that although group ($< 1-1$) is said to flatten at x_{st} equal to 4.72 mm (0.186 in) (its free height), it will actually deflect to 5.3 mm (0.21 in), where stage zero intersects stage one, before flattening because of the distributed deflection.

3. Experimental method

Carbon fiber/epoxy composite springs were fabricated using the Toray T700SC-12K-50C fiber with #2510 epoxy resin (Toray Industries; Chuo, Japan). The material was procured as a pre-impregnated (prepreg) plain weave (0-90° orientation) sheet form possessing an area weight of 190 g/m². This material's elastic properties were measured using the procedures in ASTM D3039 (ASTM 2007) on flat plates tested in the axial and transverse directions (Table 1). The plates were manufactured using a similar procedure to that used in the manufacturing of the disks. The properties obtained from the coupon specimens are used for the validation of the analytical method presented. The prepreg was cut into donut-shaped pieces with inner and outer diameters of 25.4 and 57.2 millimeters (1.00 and 2.25 inches), respectively, as shown in Fig. 5: (a) The eight layers were then collated as shown in along the 0° axis; (b) Each stack was then placed in one of the aluminum molds for curing; (c) The aluminum mold allowed for a 10 degree incline. Twenty springs were cured at a time; (d) The composite prepreg disks were cured using a press-claving approach where uniform heat and pressure are applied per the recommended 121°C (250°F) cure cycle. The springs were then removed from the molds (e-f) and machined to their nominal inner and outer diameters of 29.2 and 55.9 mm (1.15 and 2.20 in), respectively.

Stacking of the disk springs in series or parallel arrangements results in variable stiffness and deflection ranges of the spring stack. Adding elements in series increases the deflection and reduces the spring rate. Adding an element in parallel increases the spring rate while keeping the same deflection. Fig. 6 shows a stack of disks along with a cross-sectional microstructure image cut radially from the outer to the inner diameter. The microstructure image shows low porosity and limited amount of fiber waviness. The compression tests on the single elements and stacks were conducted by compressing a spring disk between two flat steel platens. Friction between the contact areas is neglected for individual tests. Four individual disk elements were tested. The compression rate was 1.02 mm/min (0.04 in/min) until the disk became completely flattened. The potential for sagging was also investigated by cycling a representative disk spring to 1334 N (300 lbf) at a rate of 0.01 Hz for 50 cycles. This compression load was approximately twice that to

Table 1 Material properties in tension of unidirectional 8 ply carbon-fiber/epoxy laminates

E_1 , GPa (Msi)	E_2 , GPa (Msi)	ν_{12}	G_{12} , GPa (Msi)	Ply thickness mm (in)
57.98 (8.41)	56.33 (8.17)	0.037	4.00 (0.58)	0.2159 (0.0085)

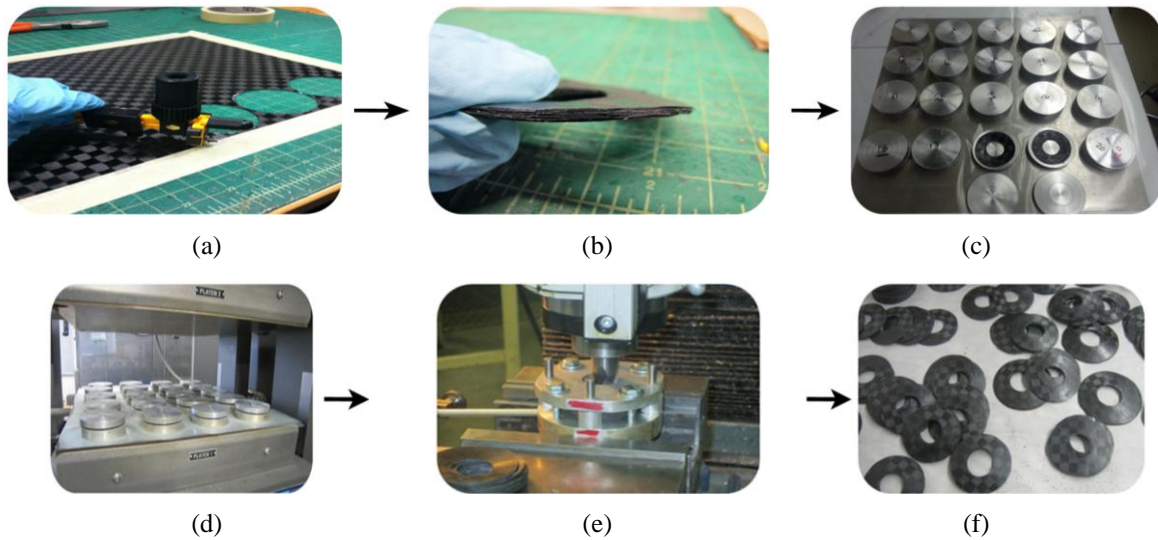


Fig. 5 Steps in fabrication of carbon-fiber/epoxy disk springs

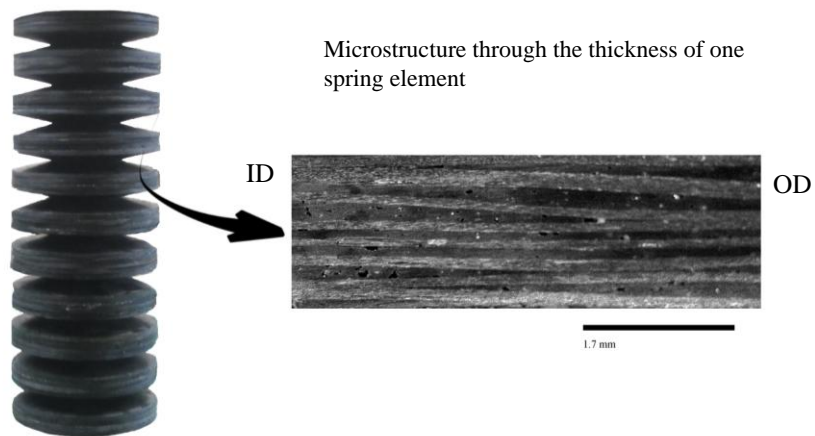


Fig. 6 Arrangement of composite disk springs in a test stack including microstructure details. In the microstructure: Left = towards inner diameter (ID); Right = towards outer diameter (OD)

create flattening and was chosen to simulate overloading. Four stack configurations were tested by switching the end disk direction.

4. Results and discussion

The theoretical model presented shows good correlation to the experimental results. The experimental results of the compression test for the individual disk springs are shown in Fig. 7. The graph contains results from four test specimens and the theoretical prediction using Eq. (9). Individual disks with similar sizes and slight geometrical differences are tabulated in Table 2.

Even though we show good correlation for this set, future investigators may wish to further examine different springs with different free heights or geometrical dimensions. From these tests shown, the spring constant was determined from the linear region of each disks load-deflection profile. The theoretical model was generated using the average dimensions from the four tested springs to ensure a repeatable representation. One theoretical prediction is included based on the average disk dimensions to illustrate the scatter in the results. In the linear region, there is little scatter and divergence, but the divergence from linearity is evident beyond the linear region. This maybe attributed to slight changes in the geometrical dimensions as noted in Table 2 and can be seen in Fig. 7. It can be seen that the theoretical predictions correlate well with the actual test data. The prediction of the maximum load shows minor divergence due to variability in the thickness of each composite disk. The analytical expression, Eq. (9) shows, a very slight change in thickness will result in a large change in the load bearing capacity. Eq. (9) is also used to investigate the effects of the free height on the load displacement relationships. This was investigated by varying the free height of five disks while holding the thickness and the inner and outer diameters constant (Fig. 8). It should be noted that although the scale is set from 0 to 2.54 millimeter (0 to 0.1 inch), the deflection to flattening of each disk is at their free height. Two types of trends can be seen in this graph; a nonlinear and linear one. When the free height is small, the disk spring will exhibit a linear load-displacement until flattening. As the free height increases, it gradually becomes more nonlinear.

Table 2 Results of single composite spring disk

Sample	ID, mm (in)	OD, mm (in)	Thickness, mm (in)	Height, mm (in)	Spring constant, N/m (lb/in)	Max Load, N (lbf)
SP#1	29.72 (1.170)	55.85 (2.199)	1.52 (0.060)	3.76 (0.1480)	465.3 (2657)	520 (117)
SP#2	29.21 (1.150)	55.79 (2.196)	1.46 (0.058)	3.73 (0.1470)	453.9 (2592)	498 (112)
SP#3	28.07 (1.105)	56.33 (2.219)	1.54 (0.061)	3.72 (0.1465)	442.0 (2524)	565 (127)
SP#4	28.27 (1.113)	56.48 (2.224)	1.46 (0.058)	3.61 (0.1420)	446.6 (2550)	485 (109)

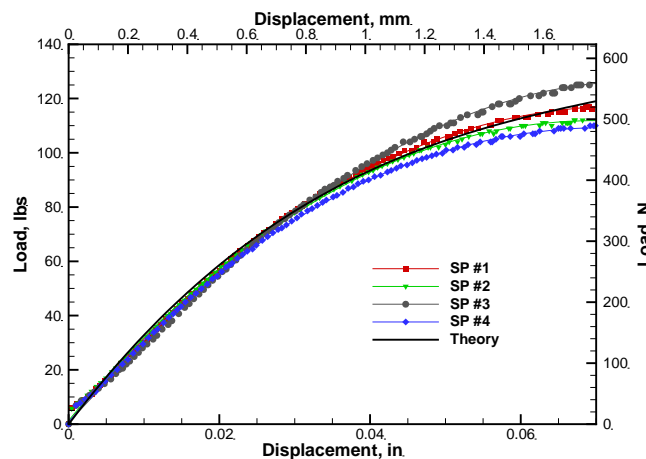


Fig. 7 Prediction of load-deflection behavior of individual disk springs elements in $[0]_8$ layup and comparison to experimental results

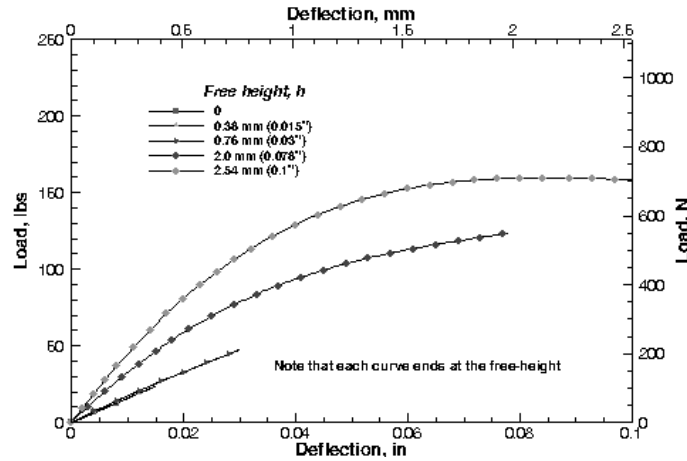


Fig. 8 Theoretical predictions of load-deflection curves with different free heights

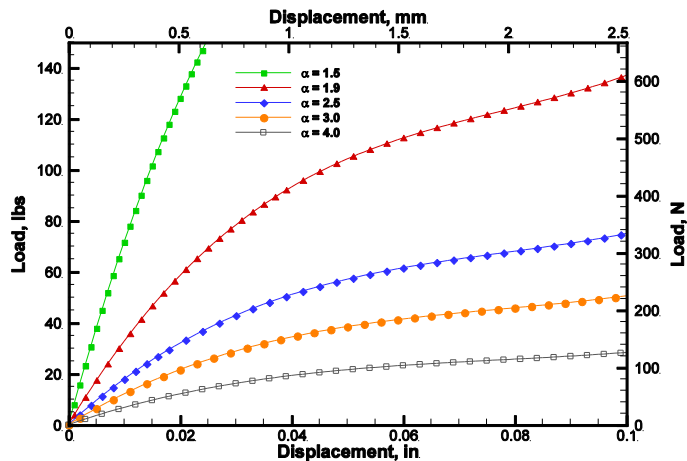


Fig. 9 Theoretical prediction of load-deflection curves for five different disk springs with different outer and inner radius properties

The effects of the geometrical influences of the diameters on the deformation response are also investigated. The theoretical load-deflection curves for five different springs with different outer diameter to inner diameter ratios, α , are shown in Fig. 9. This ratio, α , was varied from 1.5 to 4.0 while the thickness and free height were held constant. The lower the outer diameter-inner diameter ratio, α , the more load a spring can carry before reaching its fully compressed height. As the ratio continues to increase, the stiffness decreases. Thus, the spring diameters are shown to offer the flexibility to alter the load-deflection properties of a spring stack.

In addition to the strength and fatigue requirements, the design of springs typically considers sagging effects. As springs sag with time, their ability to support the required forces is reduced. After initial loading, there is an offset in the displacement that can be attributed to sagging. The initial cycle induces some sagging, but this effect is diminished as further cycling is introduced as shown in Fig. 10. This may indicate that disc springs may need to be readjusted after some amount

Table 3 Behavior of spring stack containing 44 disks in series and parallel

	Theoretical	Actual	% Error
Stack height, mm (in)	129.03 (5.080)	123.90 (4.878)	3.98 %
Spring constant, kN/m (lbf/in)	43.72 (249.64)	43.42 (247.92)	0.69 %

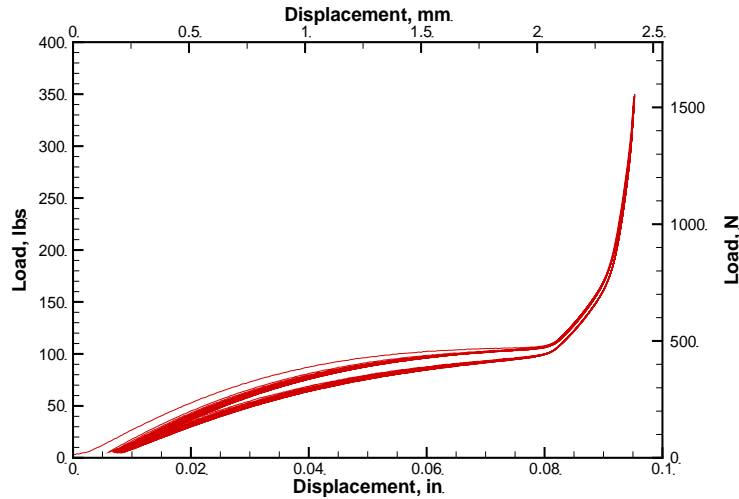


Fig. 10 Experimental results of sagging behavior of a typical composite disk spring

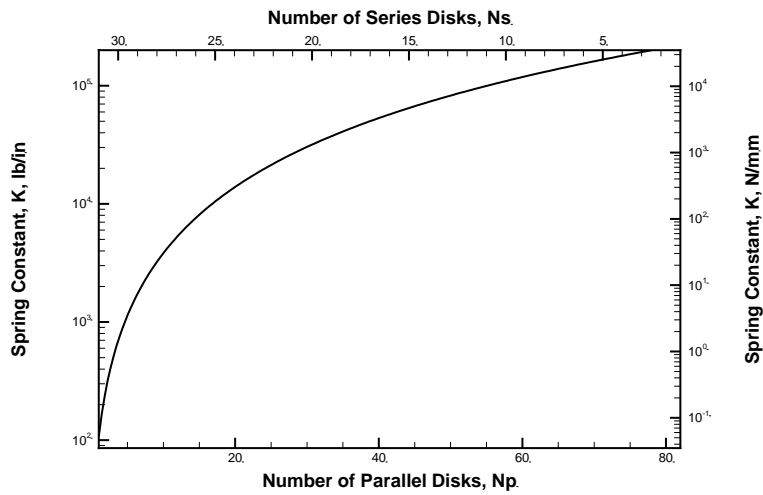


Fig. 11 Spring constant curve for 127 mm (5 in.) stacks with all equal groupings of parallel-series combinations

of cycling to make sure the sagging effect is reduced. This is consistent with various studies that have considered the viscoelastoplastic behavior of composite materials including the Baushinger effects (Lee *et al.* 2004, Saleeb *et al.* 2003). The curves do not show a diminishing the stiffness response for the limited number of cycles considered. The analytical relationships for stack

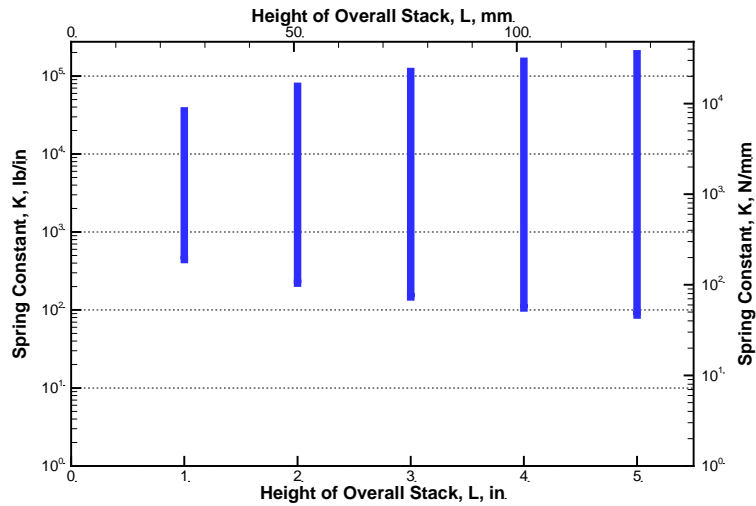


Fig. 12 Spring constant ranges as a function of stacking height

behavior were also investigated in the case of stacks containing multiple stage deformation behaviors. When determining the stack sequence for application, the spring is likely confined to a predetermined length. In these situations, having a wide range of spring constants is a huge benefit of disks springs. To demonstrate the variable stiffness values available within a given length of spring, Eqs. (12) and (13) were used to determine the theoretical spring constant ranges. The equations use only equal groups of parallel units. A stack containing 2 disks per unit and 22 units total was tested. The stack was loaded under compression and the linear spring constant was obtained from the linear slope of the load-deflection curve up to a deflection of 0.05 mm. The results of these measurements are shown in Table 3. The actual spring constant and theoretical

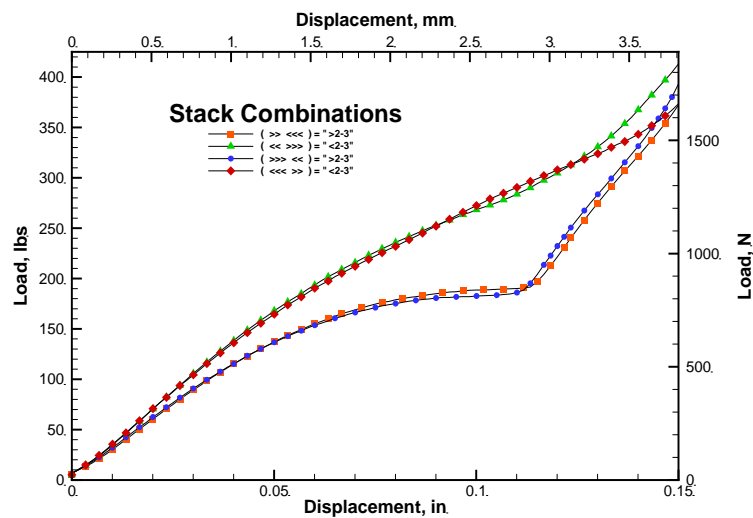


Fig. 13 Load-deflection curves for “2-3” parallel-series stack combinations

spring constant show good agreement. In addition to these results, a combination of elements in parallel and series were compared to evaluate the stack stiffness. Fig. 11 shows the spring constant variation for an overall stack height of 127 mm (5.0 in) as a function of the number of parallel and series disk selection. Similar curves were created for 25.4, 50.8, 76.2, and 101.6 mm (1.0, 2.0, 3.0, and 4.0 in) stack heights. These results are shown in bar form in Fig. 12 to indicate the large range of spring constants possible for each given spring length. It is believed that such presentation can be used in aiding the selection of disk springs for a given application. Different materials, layups, thicknesses and ply directions offer additional spring constant ranges and curves within each length specification.

The stacking order of the disk springs was also investigated experimentally and correlated to the theoretical approach. The following stacking orders were fully compressed and plotted in Fig. 13 for comparison: ($\ll \gg$), ($\lll \gg$), ($\gg \lll$), and ($\ggg \ll$). The results show that the

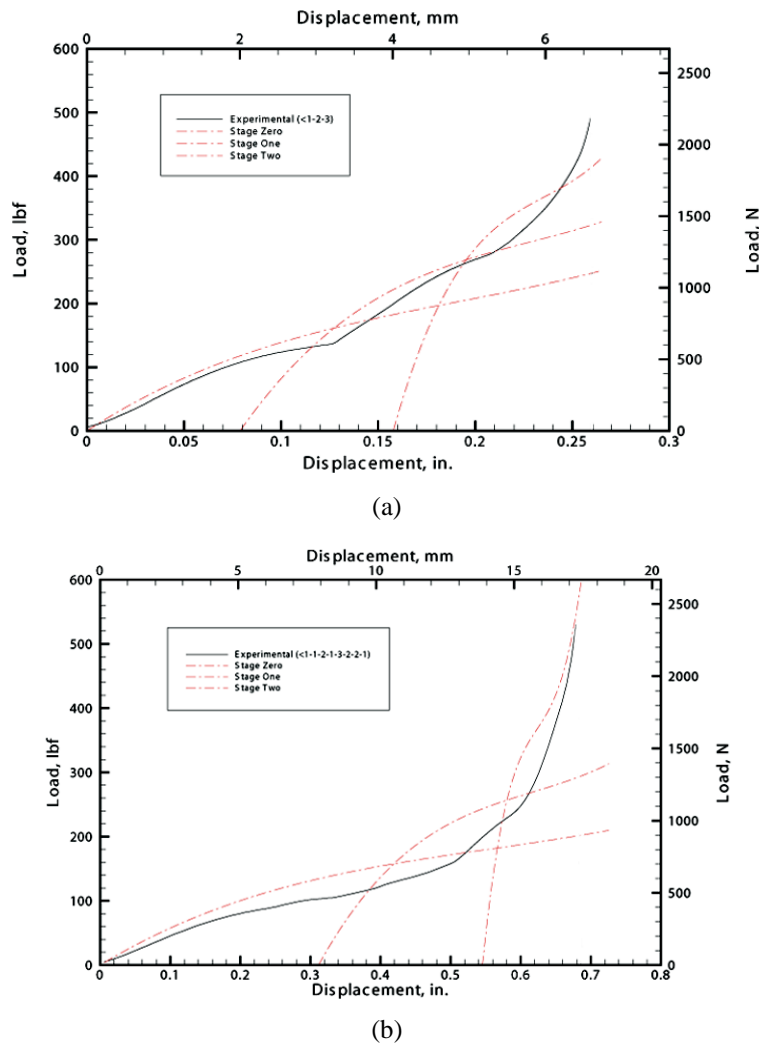


Fig. 14 Prediction of nonlinear behavior of a composite disk stack using the enveloping method

loading sequence (3 springs on top or 2 springs on top) had limited effect on the curves. The orientation of the parallel groups with respect to one another, however, did prove to alter the loading curve. For this reason, the orientation of the groups is indicated using “<” and “>” as described in Step 2 of the stack notation process. The bottom up notation creates a more universal naming and shows a consistent response. The proposed models are also used to verify the behavior in irregular stacking of disk springs. The models and experiments were performed on two stacking configurations. The two different stacks were shown in the Fig. 14(a) (< 1-2-3) and Fig. 14(b) (< 1-1-2-1-3-2-2-1) arrangements. The test data is plotted with the theoretical predictions using Eqs. 14 and 17. The theoretical predictions use the three intersecting lines which represent each compression stage. The number of stages is always equal to the number of *types* of units within a stack as previously described. The stage zero line starting at 0 mm is the average load-displacement profile of all the units in the stack. Stage one is the average profile of the units containing 2 and 3 elements. Stage 2 consists of the units with 3 elements only. The proposed approach of enveloping the results from the compression stages of the different groups shows good correlation to the experimental results. Assuming the linear dependency between the unit and the stack stiffness may be the cause of some of the variations observed. The stiffness term in Eq. 14 assumes that the ratio of deflection of each unit with respect to the entire stack remains constant. However, the stiffness of a unit will become non-linear as more load is applied. However, for most practical purposes, the springs are typically stressed in their linear region and the above assumptions shows reasonable approximation with the experimental response.

5. Conclusions

This research presents an analytical and experimental study in the behavior of specially orthotropic disk springs and stacks. An analytical approach is presented for predicting the deformation behavior of disk springs of specially orthotropic laminates with arbitrary geometric parameters. The study also investigated a methodology for obtaining the deformation behavior of a stack of disk springs directly accounting for the different stages of deformation. A naming convention was also introduced to clearly describe a stacking sequence for handling stacks with large numbers of disk elements. The stack naming is critical as testing indicated that the orientation of the parallel spring units can change the load-displacement behavior. The methods proposed are capable of accounting for parallel and series arrangements of uniform and irregular stacks. The methods were validated using experimental results from single element and uniform and irregular stack assemblies. The curves on the sagging behavior do not show a diminishing the stiffness response for the limited number of cycles considered. However, it is recommended that future studies consider the effects of fatigue on this behavior. The springs considered carry lower amounts of strain to become fatigue critical. Nonetheless, interaction at the boundaries and contact stresses may influence the fatigue behavior. The approach presented allows significant flexibility in the spring constant ranges by altering the outer diameter to inner diameter ratios, free height, ply direction, disk angle and number of layers for each individual disk. The stacking arrangement and unit grouping offer further flexibility.

Acknowledgments

The research described in this paper was financially supported by the National Institute of

Aerospace, Hampton, Virginia, USA.

References

- Almen, J. and Laszlo, A. (1936), "The uniform-section disk spring", *Trans. ASME*, **58**, 305-314.
- ASTM (2007), D3039, Standard test method for tensile properties of polymer matrix composite materials, ASTM International, West Conshohocken, PA, USA..
- Çalim, F.F. (2009), "Dynamic analysis of composite coil springs of arbitrary shape", *Compos. Part B: Eng.*, **40**(8), 741-757.
- Chiu, C.-H., Tsai, K.-H., Lee, Y.-C. and Hwan, C.L. (2009), "The effects of hybrid laminate structures on the compression and fatigue properties of helical composite springs", *J. Adv. Mater.*, **41**(3), 57-69.
- Cho, J., Lee, J., Kim, K. and Lee, S.B. (2013), "Generalized evolutionary optimum design of fiber-reinforced tire belt structure", *Steel Compos. Struct., Int. J.*, **15**(4), 451-466.
- Curti, G. and Montanini, R. (1999), "On the influence of friction in the calculation of conical disk springs", *J. Mech. Des.*, **121**(4), 622.
- Curti, G. and Raffa, F. (1992), "Material nonlinearity effects in the stress analysis of conical disk springs", *J. Mech. Des.*, **114**(2), 238-244.
- Dharan, C. and Bauman, J.A. (2007), "Composite disc springs", *Compos. Part A: Appl. Sci. Manuf.*, **38**(12), 2511-2516.
- Hendry, J. and Probert, C. (1986), "Carbon fibre coil springs", *Mater. Des.*, **7**(6), 330-337.
- Huchette, P.V. and Hall, Jr. H.H. (1976), Composite material springs and manufacture; United States Patent.
- Hwan, C.-L., Chiu, C.-H., Lee, W.-L. and Lee, W.P. (2010), "The effects of rubber core diameter and the number of braided outer layers on the compression and fatigue properties of helical composite springs", *J. Adv. Mater.*, **42**(1), 65-77.
- Lee, M., Kim, D., Chung, K., Youn, J.R. and Kang, T.J. (2004), "Combined isotropic-kinematic hardening laws with anisotropic back-stress evolution for orthotropic fiber-reinforced composites", *Polym. Polym. Compos.*, **12**(3), 225-233.
- Mahdi, E., Alkoles, O., Hamouda, A., Sahari, B.B., Yonus, R. and Goudah, G. (2006), "Light composite elliptic springs for vehicle suspension", *Compos. Struct.*, **75**(1-4), 24-28.
- Mallick, P. (1985), "Design and development of composite elliptic springs for automotive suspensions", *The Society of the Plastics Industry, Inc.*, 5.
- Naderi, A.-A., Rahimi, G.-H. and Arefi, M. (2014), "Influence of fiber paths on buckling load of tailored conical shells", *Steel Compos. Struct., Int. J.*, **16**(4), 375-387.
- Saleeb, A., Wilt, T., Al-Zoubi, N. and Gendy, A.S. (2003), "An anisotropic viscoelastoplastic model for composites - sensitivity analysis and parameter estimation", *Compos. Part B: Eng.*, **34**(1), 21-39.
- Schnorr (2003), Handbook for Disc Springs, Ann Arbor, MI, USA.
- Scowen, G. and Hughes, D. (1985), "The sulcated spring", (*International Seminar*) *Proceedings of Autotech 85 Congress*, The Institution of Mechanical Engineers; Automobile Division, IMechE publications.
- So, C., Tse, P., Lai, T. and Young, K.M. (1991), "Static mechanical behaviour of composite cylindrical springs", *Compos. Sci. Technol.*, **40**(3), 251-263.
- Subramanian, C. and Senthilvelan, S. (2011), "Short-term flexural creep behavior and model analysis of a glass-fiber-reinforced thermoplastic composite leaf spring", *J. Appl. Polym. Sci.*, **120**(6), 3679-3686.
- Suprith, N., Annamalai, K., Naiju, C. and Mahadevan, A. (2013), "Design and analysis of automotive multi-leaf springs using composite materials", *Appl. Mech. Mater.*, **372**, 533-537.
- Thompson, J., Marshall, I., Wood, J. and Hendry, J.C. (1992), "Computer aided design of FRP sulcated springs", *Computer Aided Design in Composite Material Technology III*, Springer, 445-462.
- Topal, U. (2013), "Pareto optimum design of laminated composite truncated circular conical shells", *Steel Compos. Struct., Int. J.*, **14**(4), 397-408.
- Tse, P., Lai, T., So, C. and Cheng, C.M. (1994), "Large deflection of elastic composite circular springs under uniaxial compression", *Int. J. Non-linear Mech.*, **29**(5), 781-798.

- Wong, W.H., Tse, P.C., Lau, K.J. and Ng, N.F. (2004), "Spring constant of fibre-reinforced plastics circular springs embedded with nickel-titanium alloy wire", *Compos. Struct.*, **65**(3-4), 319-328.
- Yu, A. and Hao, Y. (2013), "Effect of warping on natural frequencies of symmetrical cross-ply laminated composite non-cylindrical helical springs", *Int. J. Mech. Sci.*, **74**, 65-72.

CC